Forest canopy recovery from the 1938 hurricane and subsequent salvage damage measured with airborne LiDAR

John F. Weishampel [a,*], Jason B. Drake [a,d], Amanda Cooper [a], J. Bryan Blair [b], Michelle Hofton [c]

[a] Department of Biology, University of Central Florida, Orlando, FL 32816-2368, USA
[b] Laboratory for Terrestrial Physics, NASA Goddard Space Flight Center, Greenbelt, MA, USA
[c] Department of Geography, University of Maryland, College Park, MD, USA
[d] USDA Forest Service, Tallahassee, FL, USA

Abstract

The structure of a forest canopy often reflects its disturbance history. Such signatures of past disturbances or legacies can influence how the ecosystem functions across broad spatio-temporal scales. The 1938 hurricane and ensuing salvage operations which swept through New England represent the most recent large, infrequent disturbance (LID) in this region. Though devastating (downing ∼70% of the timber at Harvard Forest), the disturbance was not indiscriminate; it left behind a heterogeneous landscape comprised of different levels of canopy damage. We analyzed large-footprint LiDAR, from the Prospect Hill tract at Harvard Forest in central Massachusetts, to assess whether damage to the forest structure from the hurricane and subsequent timber extraction could be discerned after ∼65 years. Differences in LiDAR-derived measures of canopy height and vertical diversity were a function of the degree of damage from the 1938 hurricane and the predominant tree species which is, in part, a function of land use history. Higher levels of damage corresponded to slightly shorter canopies with a less even vertical distribution of return from the ground to the top. In addition, differences in canopy topography as revealed by spatial autocorrelation of canopy top heights were found among the damage classes. Less disturbed stands were characterized by lower levels of local autocorrelation for canopy height and higher levels of vertical diversity of LiDAR returns. These differences in canopy structure reveal that the forest tract has not completely recovered from the 1938 LID and salvage regime, which may have implications on arboreal and understory habitat and other ecosystem functions.
© 2007 Elsevier Inc. All rights reserved.

Keywords: Disturbance; Ecosystem recovery; Forest canopy; Harvard Forest; Hurricane; Land use; Legacy; LiDAR; LISA; Spatial autocorrelation; Vertical structure

1. Introduction

Large, infrequent disturbances (LIDs) bestow spatially extensive imprints on forested ecosystems that may persist for decades to centuries (Turner & Dale, 1998). LIDs often vary in intensity leaving behind differential biotic legacies such as coarse woody debris, snags, and surviving trees (Keeton & Franklin, 2005). The ecological consequences of major disturbances are often misunderstood by policy-makers and natural resource managers which may yield decisions that undermine the benefits of processes associated with natural ecosystem recovery (Lindenmayer et al., 2004). Catastrophic winds from hurricanes, an example of a LID, create damage patterns that are a function of spatially variable abiotic (e.g., topographic exposure, soil moisture, wind gradients) and biotic (e.g., tree species and height distribution) conditions (Boose et al., 1994, 2001; Foster, 1988; Foster & Boose, 1992; McMaster, 2005) producing structural complexity across the landscape. Residuals may influence secondary succession and their diversity, leading to the generation of additional heterogeneity (Franklin et al., 2002; Palik & Robl, 1999; Turner et al., 1998). Furthermore, because tree species are long-lived, the present structure of a forest may represent single or multiple states of recovery from prior disturbances (Merrens & Peart, 1992).

The forest canopy serving as the interface between the atmosphere and the biosphere, has been compared to a membrane (Birnbaum, 2001) functioning as the master regulator of the forest (Hallé et al., 1978); its structure, in large part, controls the biophysical environment influencing tree physiology,

atmospheric exchange and biotic habitat (Frazer et al., 2005; Nadkarni et al., 1996). Though frequent wind disturbance may create conditions that mold canopy structure (Foster et al., 1998), existing canopy structure may also reflect the historical consequences of infrequent disturbances. The surface topography (Cohen et al., 1990; Weishampel et al., 1992) and the internal structure (i.e., canopy profiles, Aber, 1979; Lefsky et al., 1999) of the canopy reflect the successional stage of the forest or the recovery time since disturbance. These canopy architectural properties, among other things, have been related to wind flow, sound and radiation transmission, and niche space (e.g., Hill et al., 2004; MacArthur & MacArthur, 1961; Parker et al., 2004; Tunick, 2003). In this study, using large-footprint, LiDAR (Light Detection and Ranging) remote sensing, we assess whether or not differences in canopy structure have persisted from decades-old (∼65 years) hurricane damage and associated salvage logging.

2. Methods

2.1. Harvard Forest study area

The area studied was the Prospect Hill Tract of the Harvard Forest in the Massachusetts townships of Petersham and Phillipston centered near 42.54 N, 72.19 W (Fig. 1a). This ∼380-ha tract ranges in elevation from 270 to 420 m a.s.l. (Harvard Forest LTER, 2005).

Ground topography measured from the laser altimeter described below revealed a varied terrain that ranged from 263 to 410 m and visually matches the 30 m USGS National Elevation Dataset available through the Harvard Forest LTER.

The Prospect Hill Tract is a patchwork landscape that has had numerous land owners since 1730 and has been subjected to a complex array of historic agricultural and logging treatments (Foster, 1992; Motzkin et al., 1999, 2004). These were largely discontinued by the time it was acquired by Harvard University as an experimental forest in 1907. Presently, it is predominantly covered by a maturing forest described as part of the transition hardwood–white pine (WP; *Pinus strobus*)–hemlock (Hem; *Tsuga canadensis*) vegetation zone of New England (Spurr, 1956a; Westveld et al., 1956). Within this matrix, there are dispersed red pine (RP; *Pinus resinosa*) and Norway spruce (NS; *Picea abies*) plantations and several bogs. Hardwood species are primarily Northern red oak (RO; *Quercus rubra*), red maple (RM; *Acer rubrum*), and black oak (BO; *Quercus velutina*). Additional dominant conifer species include white spruce (WS; *Picea glauca*) which are often planted in this area.

In addition to varied land-use practices, the Prospect Hill tract has been exposed to wind, fire, ice, snow, and pathogen disturbances. The most devastating in recent history was the 1938 September 21st hurricane which led to a reduction of 70% of the standing timber volume at Harvard Forest (Foster, 1988; Foster & Boose, 1992; Spurr, 1956b). On Prospect Hill there were different degrees of severity (Table 1), 61% of the tract area (54% of the stands) lost 1–50% of its overstory while 22% (31% of the stands) lost >50% (Motzkin et al., 2004). The severity of impact for particular stands were related to species composition, height, and topographic position related to wind exposure (Foster, 1988; Foster and Boose, 1992). Immediately following the hurricane, to reduce the threat of fire, Harvard Forest became part of the largest salvage operation in U.S. history. Damaged and uprooted trees were cut and removed
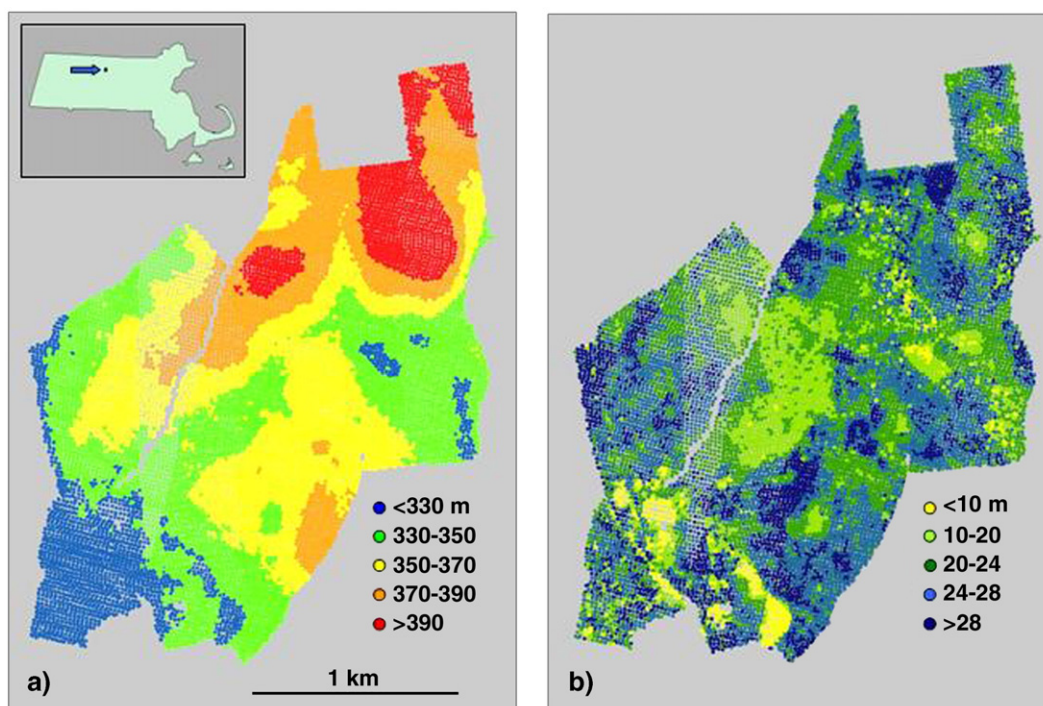

Fig. 1. LiDAR-derived measures of (a) ground topography and (b) canopy top height from the Prospect Hill tract of Harvard Forest located in the Petersham and Phillipston townships in central Massachusetts (designated by the arrow in the inset).

Table 1
Species composition in damage class polygons

Damage class	Area (ha)	Stand count	Footprint count	Predominant species (% by area)							
				BO	RM	RO	Hem	NS	RP	WP	WS
Und	42.87	36	2739	5.3	12.4	38.9	1.1	4.5	8.1	19.6	6.0
VSD	52.36	40	2972	0.6	18.3	32.0	7.1	0.8	24.9	5.8	6.8
MD-1	72.72	44	4052	0.0	15.6	41.0	24.1	2.5	6.1	5.6	0.6
MD-2	70.34	46	3778	2.4	19.7	20.3	21.4	0.1	6.2	10.8	0.5
SD-1	32.91	24	2223	11.6	16.6	37.9	14.5	0.4	1.3	15.9	0.1
SD-2	15.66	20	889	0.0	19.3	34.1	4.3	0.0	1.3	27.7	0.2
Des	17.59	32	972	12.7	24.1	31.2	2.3	0.8	0.5	18.2	3.2
			Footprint count	754	3222	5914	3185	363	1578	2122	487
			Stand count	2	46	59	20	4	27	31	13
			Area (ha)	10.7	69.1	104.5	42.6	4.6	26.4	43.5	8.1

Damage and predominant species stand numbers and areas represent polygons that intersect one another from Fig. 3.

Note: black oak (BO), red maple (RM), northern red oak (RO), hemlock (Hem), red pine (RP), white pine (WP), white spruce (WS).

further opening the forest canopy (Foster et al., 2004). Remaining slash was piled and burned modifying the underlying soil and adding to hurricane effects. Hence, the hurricane can be equated to a broad-scale logging operation (Foster et al., 1997) followed by natural restocking and secondary succession (Spurr, 1956b). Roughly 50 years after the disturbance, overstory tree composition returned to some semblance of its pre-hurricane composition (Mabry & Korsgren, 1998). Silvicultural treatments on Prospect Hill subsequent to the hurricane including thinning, improvement cutting, small clearcutting, and additional salvage logging from fire and blowdown damage occurred sporadically and were not very extensive across the landscape.

2.2. Acquisition of LiDAR data

In July 2003, during the midst of the growing season, roughly 65 years after the 1938 hurricane, NASA's Laser Vegetation Imaging Sensor (LVIS; Blair et al., 1999) acquired data from Harvard Forest tracts and adjacent areas in central Massachusetts. LVIS consists of a scanning airborne laser altimeter combined with an inertial navigation system and global positioning system that enables the collection of georeferenced, digitally-recorded waveforms to simultaneously measure slightly off-nadir-projected distribution of forest canopy surfaces and ground topography. For these overflights, the nominal ground footprint diameter was 20 m. Footprint spacing was contiguous; the center of each footprint was separated by roughly 20 m both across and along the flight path. Footprint track widths varied between 1600 and 2000 m depending on aircraft altitude. Several passes were made to thoroughly blanket the landscape within a 2-km radius circle centered on the CO_2 flux tower in the hemlock stand on the Prospect Hill tract. As a result, the final coverage in this area was considerably denser and significantly clustered; average nearest neighbor distances between footprint centers on the Prospect Hill tract was 7.1 m. For this study, the data used from this mission included the longitude and latitude of the footprint center; the ground elevation and canopy top height within a footprint; and the vertical distribution of intercepted surfaces within a footprint (i.e., the waveform) with a vertical resolution of 0.3 m (Blair et al., 2004).

2.3. Derivation of canopy properties

Though ground topography sometimes can influence large footprint waveform properties, affecting estimates of canopy top height (Hofton et al., 2002; Hyde et al., 2005; Lefsky et al., 2005), the terrain at the Harvard Forest is not sufficiently rugged to alter the waveform shape appreciably. Canopy top height (CH; Fig. 1b) was calculated as the height in meters relative to the mean elevation of the lowest detected mode within the waveform at which 100% of the waveform energy occurs (see diagram in Hyde et al., 2005). Previous studies of large footprint LiDAR show very close agreement with field- and LiDAR-derived (i.e., LVIS and Scanning LiDAR Imager of Canopies by Echo Recovery — SLICER) ground elevations (Hofton et al., 2002) and canopy heights (e.g., Boutet and Weishampel, 2003; Hyde et al., 2005; Lefsky et al., 1999). For similar New England forests, a strong correlation ($r^2 = 0.80$) between field- and LVIS-derived heights exists (Anderson et al., 2006).

To further explore potential effects of hurricane disturbance on vertical canopy structure, we analyzed the waveforms from the different damage classes. This represents the vertical organizational patterns below the outer canopy surface found within a footprint. A canopy height diversity index (CD), which uses a Shannon index mimicking the foliage height diversity index (FHD; Aber, 1979; Hashimoto et al., 2004; MacArthur & MacArthur, 1961; McElhinny et al., 2005) similar to another canopy height diversity index (CHD; Spies & Cohen, 1992), was used to measure the distribution of laser returns within the 0.3 m bins from the ground to the canopy top.

$$CD = \sum_{i=1}^{s} p_i \ln p_i \qquad (1)$$

where p_i is the proportion of return in one of s vertical bins in which there was a laser return recorded above the background noise. Because the laser reflects off of the surfaces of all canopy components (i.e., leaves, twigs, branches, boles, etc.) not just foliage, the acronym, FHD, was modified following Lefsky et al. (1999). As FHD tends to be highly correlated with canopy height (Aber, 1979) or the number of layers or bins (Parker & Brown, 2000; Unruh, 1991), so should CD. To remove some of
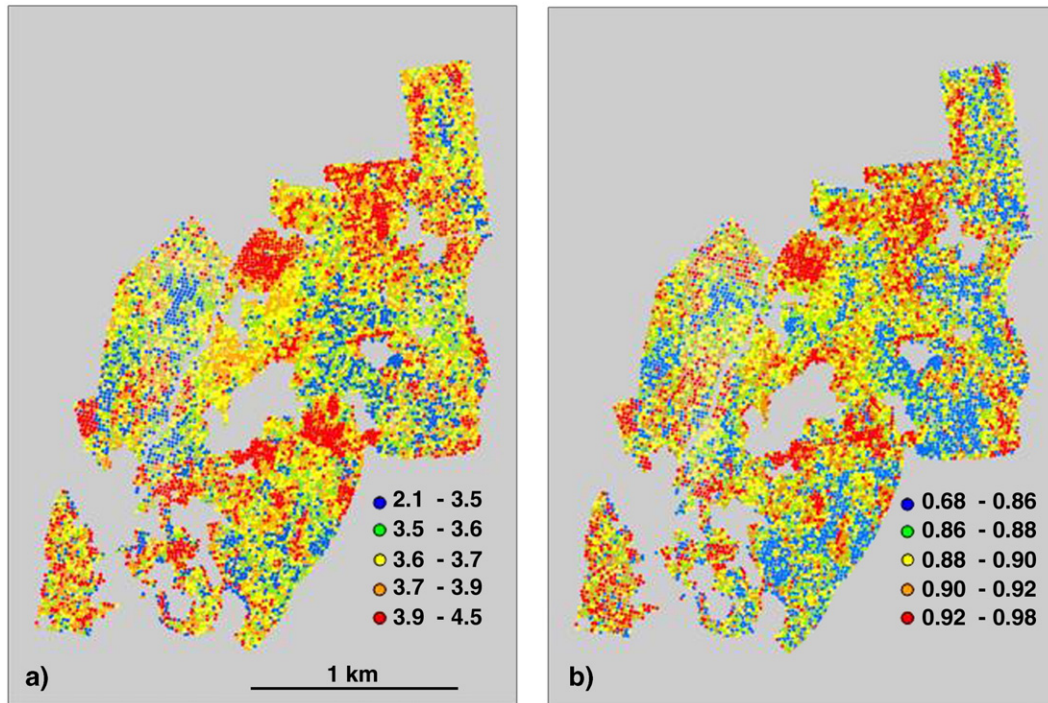
Fig. 2. LiDAR-derived measures of (a) canopy diversity (CD) and (b) canopy evenness (CE) from the Prospect Hill tract at Harvard Forest. Colors are scaled based on quantiles of the range of measurements. (For interpretation of the references to color in this figure legend, the reader is referred to the web version of this article.)

these biases, we created a canopy evenness index (CE) which assumes values between 0 and 1 by dividing CD by the natural logarithm of s (following ecological measures of species evenness, e.g., Smith and Wilson, 1996). This index ranges between 0 and 1. Measures of CD and CE across the Prospect Hill landscape are shown in Fig. 2.
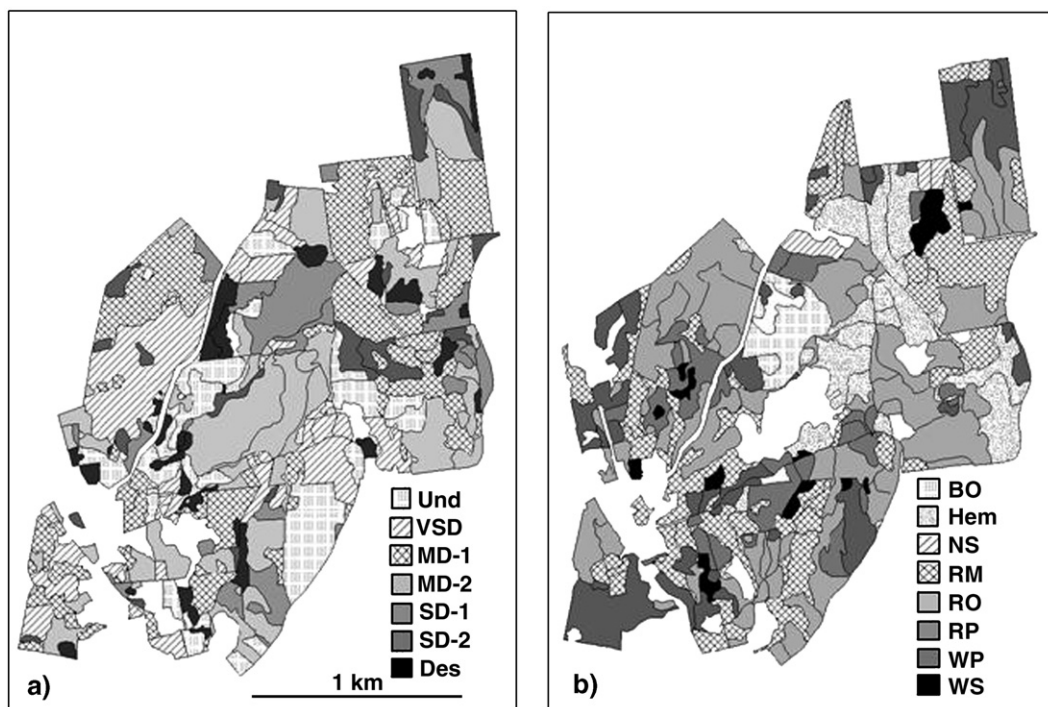

Fig. 3. (a) Canopy damage class polygons from the 1938 hurricane from the Prospect Hill tract at Harvard Forest. Open areas are not included. (b) Predominant species polygons from the Prospect Hill tract from the 1986–1993 survey of Harvard Forest. Wetlands and small polygons representing other dominant species are not included.
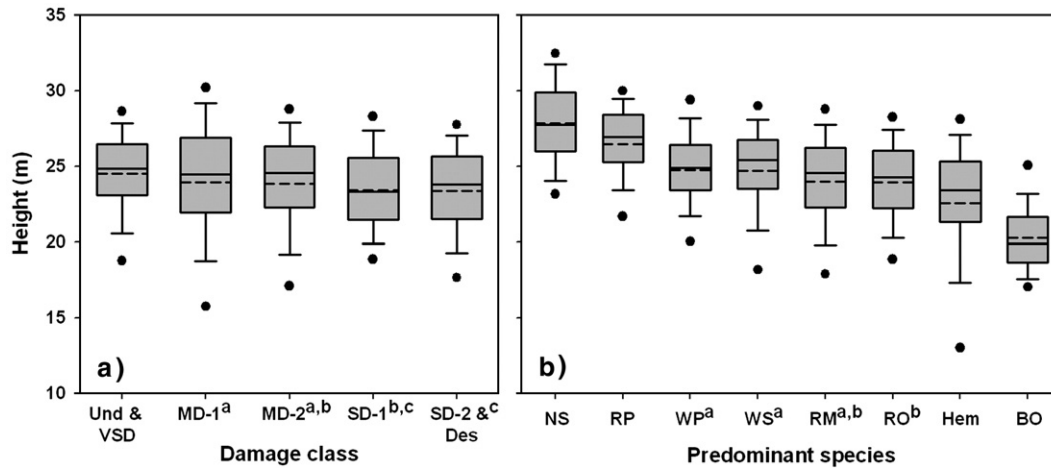
Fig. 4. LiDAR-derived measures of canopy top height from tall to small for the different (a) damage class and (b) predominant species polygons from the Prospect Hill tract. Dashed lines represent average values. Solid lines in boxes represent median values. Edges of boxes represent 25th and 75th percentiles. Whisker bars represent 10th and 90th percentiles. Circular markers represent 5th and 95th percentiles. For a given panel, different superscripts adjacent to class label indicate statistically different values ($P<0.05$ based on Duncan's post hoc test).

2.4. Comparison with GIS datalayers

We compared measures of canopy height, diversity, and evenness derived with LVIS among different hurricane damage and predominant species classes using ANOVA and General Linear Model (GLM) approaches. LiDAR measurements of CH are typically spatially autocorrelated at fine scales (Boutet & Weishampel, 2003; Drake & Weishampel, 2000; Weishampel et al., 2000) and represent organizational patterns at the crown and crown neighborhood level. Because autocorrelation violates the assumption of independence among samples, it can elevate statistical errors (Legendre, 1993; Popescu et al., 2004). To reduce this effect, we generated a 25 m triangular lattice across the study area. Canopy height, diversity, and evenness, measures from the footprints closest to the lattice points, were analyzed. This sampling scale was greater than the footprint diameter of LVIS (~20 m) and the crown diameter of trees in this region (Leak, 1983), thus should prevent repeated sampling of the same tree. This sampling method resulted in the elimination of about two-thirds of the footprints.

Hurricane damage assessment data for the forests around Petersham, Massachusetts were collected between 1939 and 1941 (Rowlands, 1941). The percent of all dominant and co-dominant trees which were uprooted, snapped, or leaning sufficiently to prevent saving as part of the residual stand were
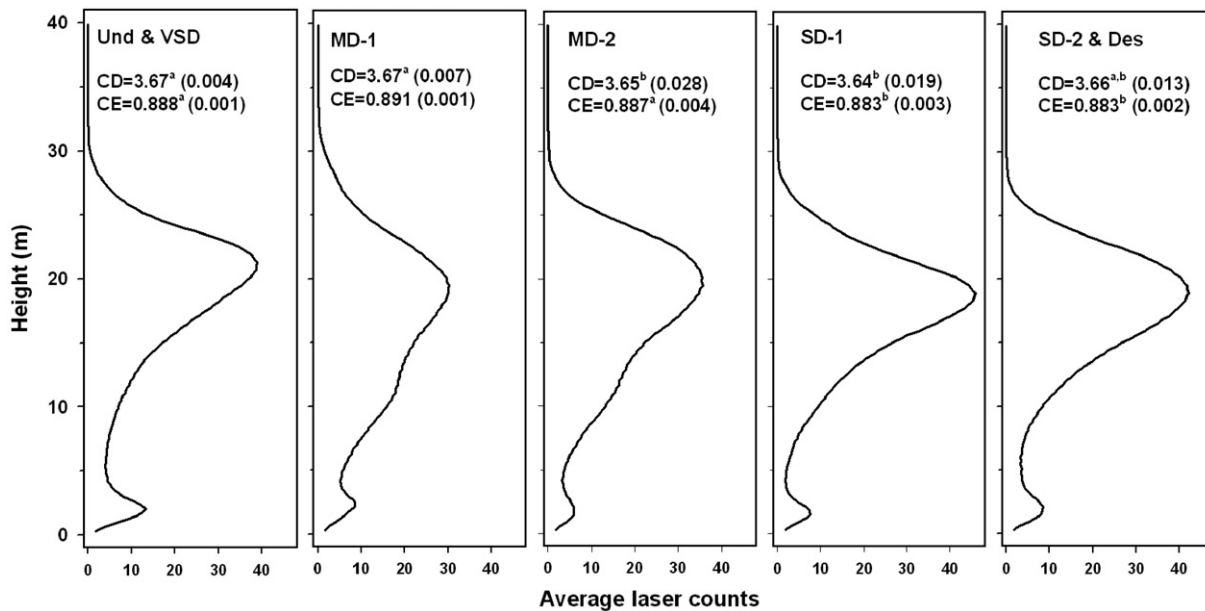

Fig. 5. Average vertical distribution of LiDAR returns (above background noise) and canopy diversity indices with standard errors in parentheses for the different damage classes. Identical superscripts adjacent to means indicate statistically similar values ($P<0.05$ based on a Duncan's post hoc test).

recorded for each stand. These areas representing ∼ 304 ha were classified into seven canopy damage classes: undamaged (Und), <11% very slight damage (VSD), 11–25% moderate damage 1 (MD-1), 26–50% moderate damage 2 (MD-2), 51–75% severe damage 1 (SD-1), 76–90% severe damage 2 (SD-2), and >90% destroyed (Des). These classes were then mapped, and digitized into a GIS datalayer of 242 separate stand polygons (Fig. 3a; Foster and Boose, 1992; Motzkin et al., 1999). To increase footprint number per damage class, the two classes representing the least amount of damage (Und and VSD) were combined as were those representing the most amount of damage (SD-2 and Des). The predominant species polygons were derived from a survey of Harvard Forest stands that occurred from 1986 to 1993 (Fig. 3b). Predominant species designations were based on basal area of living, not moribund, stems. Little change was expected in the predominant species class a decade later when the LVIS flights occurred. The proportion of species dominating a particular damage class is shown in Table 1. GIS datalayers are available through the Harvard Forest Long Term Ecological Research (LTER) archives.

2.5. Measures global and local autocorrelation

Though spatial autocorrelation violates assumptions of independence for hypothesis testing, it may provide important information on the structural organization of a system (Legendre, 1993). To quantify differences in canopy topography that may reflect structural legacies from the 1938 hurricane, we generated spatial correlograms of CH for the different damage classes. Measures of autocorrelation such as semivariance are essentially textural measures (Dale et al., 2002) and have been used to help visualize and quantify forest canopy structure (e.g., Cohen et al., 1990; Tian et al., 2002; Weishampel et al., 1992, 2000) and assess damage (Bowers et al., 1994; Lévesque & King, 1999; King et al., 2005). As in a previous study (Boutet & Weishampel, 2003), we used Moran's I to quantify autocorrelation globally. Across a range of lag distances at 10 m intervals, this autocorrelative measure was used to produce a correlogram using GS+ v. 7.0 software (Gamma Design, 2005). These results range between 1.0 and −1.0 and are interpreted in a similar fashion as a Pearson's Product Moment correlation statistic. We generated
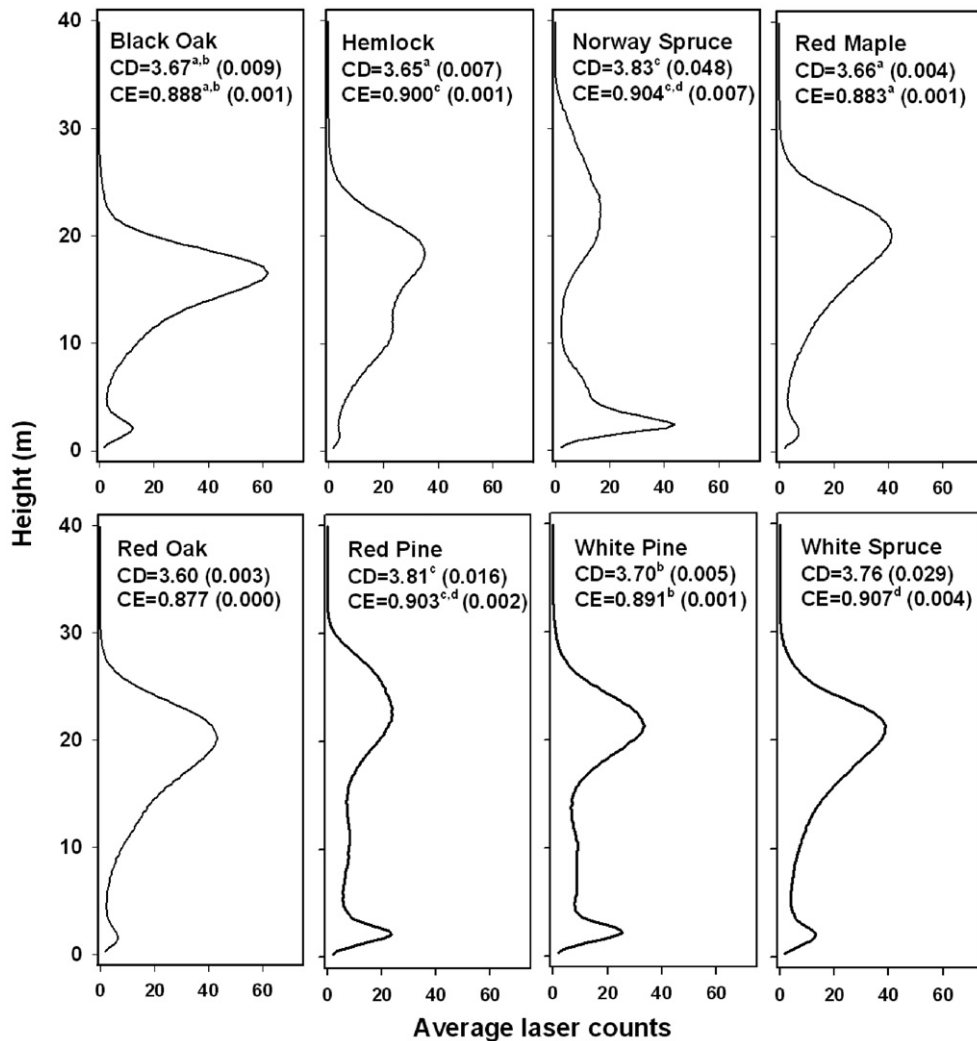

Fig. 6. Average vertical distribution of LiDAR returns (above background noise) and canopy diversity indices with standard errors in parentheses for the different predominant species classes. Identical superscripts adjacent to means indicate statistically similar values ($P<0.05$ based on a Duncan's post hoc test).

correlograms for different damage and predominant species classes with sufficient LiDAR sampling (i.e., the five damage and five species classes with >1000 footprints) to allow numerous comparisons across lag scales ranging between 5 and 250 m.

Because global measures of autocorrelation often mask fine-scale patterns within a single metric or across a given range of lag distances (Wulder & Boots, 2001), we also used a local indicator of spatial association (LISA) to quantify autocorrelation at the footprint scale. These local measures provide an assessment of how each observation contributes to global autocorrelation measures and can be used to identify pockets

(hotspots) of stationarity and nonstationarity. We used the Local Moran statistic I_i (Anselin, 1995):

$$I_i = \frac{Z_i - \bar{Z}}{S^2} \sum_{j=1}^{N} W_{ij}(Z_j - \bar{Z}) \qquad (2)$$

where $\bar{Z}$ is the mean intensity over all observations, Z_i and Z_j are the intensities of observations i and j, respectively (where $i \neq j$), S^2 is the variance over all observations, and W_{ij} is a distance weight for the interaction between observations i and j (Getis and Ord, 1996; Levine, 2004). Unlike the global Moran's I, the
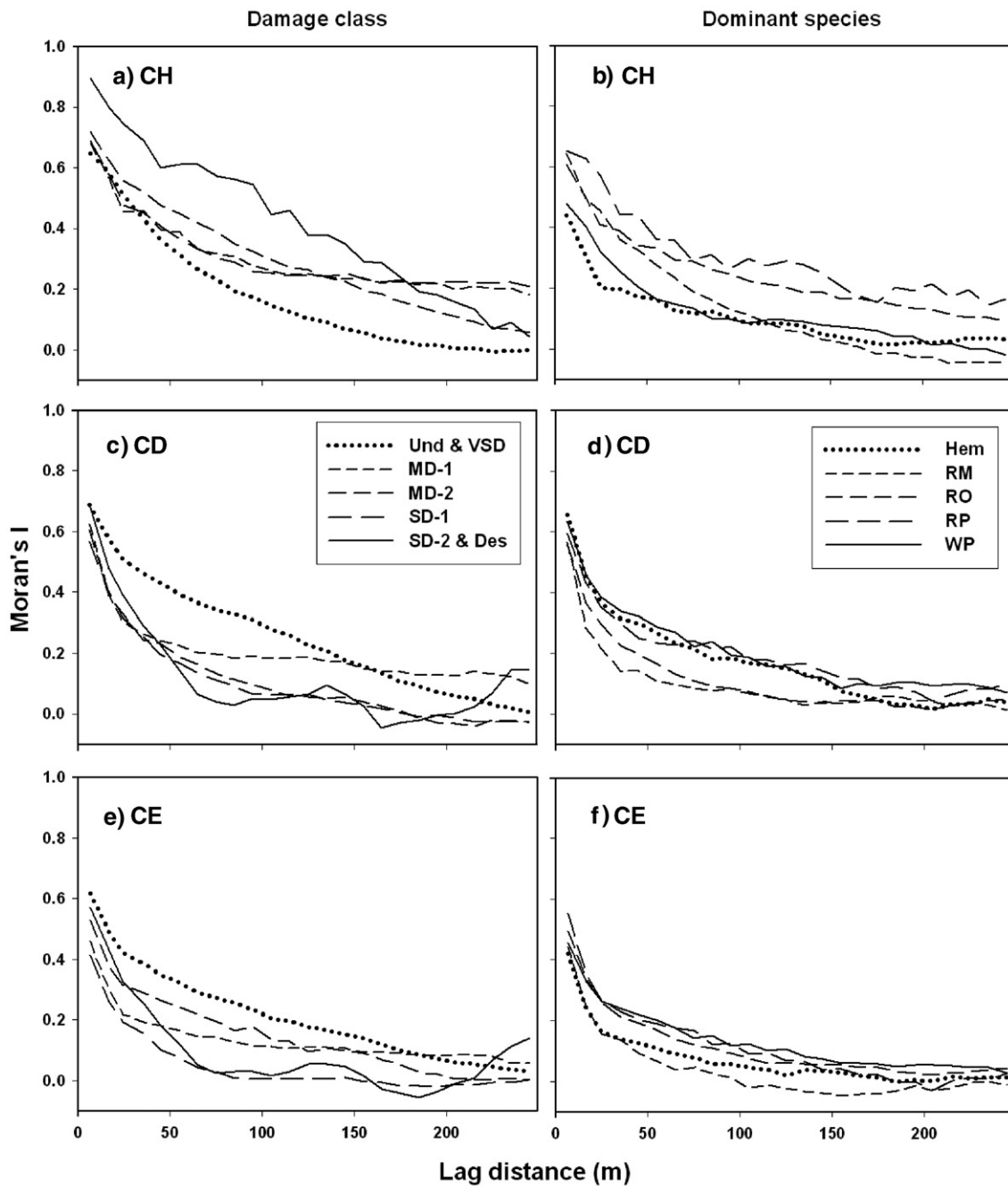

Fig. 7. Correlograms for LiDAR-derived measures of canopy surface topography (CH), diversity (CD), and evenness (CE) for the different damage class (left) and predominant species (right) polygons from the Prospect Hill tract.

distribution of I_i is unknown. High positive or negative values indicate the spatial clustering of similar or dissimilar values, respectively, within a neighborhood. Though knowledge of the distribution of LISA measures is incomplete (Boots, 2002), we ran significance tests as part of exploratory data analysis. For each polygon designated by damage and dominant species class, I_i values were averaged. At the polygon level these were compared to determine whether or not differences exist for LISA measures using ANOVA and GLM methods.

3. Results

3.1. Differences in canopy architecture

Measures of CH significantly decreased as hurricane impact increased (Fig. 4a). The tallest canopies were in the aggregated undisturbed and very slightly disturbed class ($z = 24.1$ m, SE = 0.62), and the shortest canopies were in the aggregated severely disturbed-2 and destroyed class ($z = 23.4$ m, SE = 0.21). Thus, the difference generated by the 1938 hurricane, though significant, was < 1 m. CH was more dramatically a function of

predominant canopy species (Fig. 4b). The two plantation classes, Norway spruce ($z = 26.2$ m, SE = 0.73) and red pine ($z = 25.9$ m, SE = 0.27) were significantly taller than the other classes. Hemlock ($z = 22.5$ m, SE = 0.10) and black oak ($z = 20.1$ m, SE = 0.14) stands were the shortest classes. When considered individually and in combination, the hurricane damage and predominant species classes contributed to significant differences ($P < 0.01$) in CH derived by the LiDAR.

Though differences in the average vertical canopy profiles are apparent (Fig. 5), the diversity indices are nearly identical among the damage classes. However, there were significant differences ($P < 0.05$) in CD with the more disturbed stands having lower values than those that experienced less damage. The CE values were significantly different showing again the more disturbed stands to have lower values. The waveforms for the different predominant species classes (Fig. 6) are much more obviously different than the damage classes. The taller, plantation classes, Norway spruce and red pine exhibited the highest CD and CE values. It is interesting to note that an understory in the hemlock class was not apparent which may reflect the low light conditions. Though we attempted to remove the canopy height
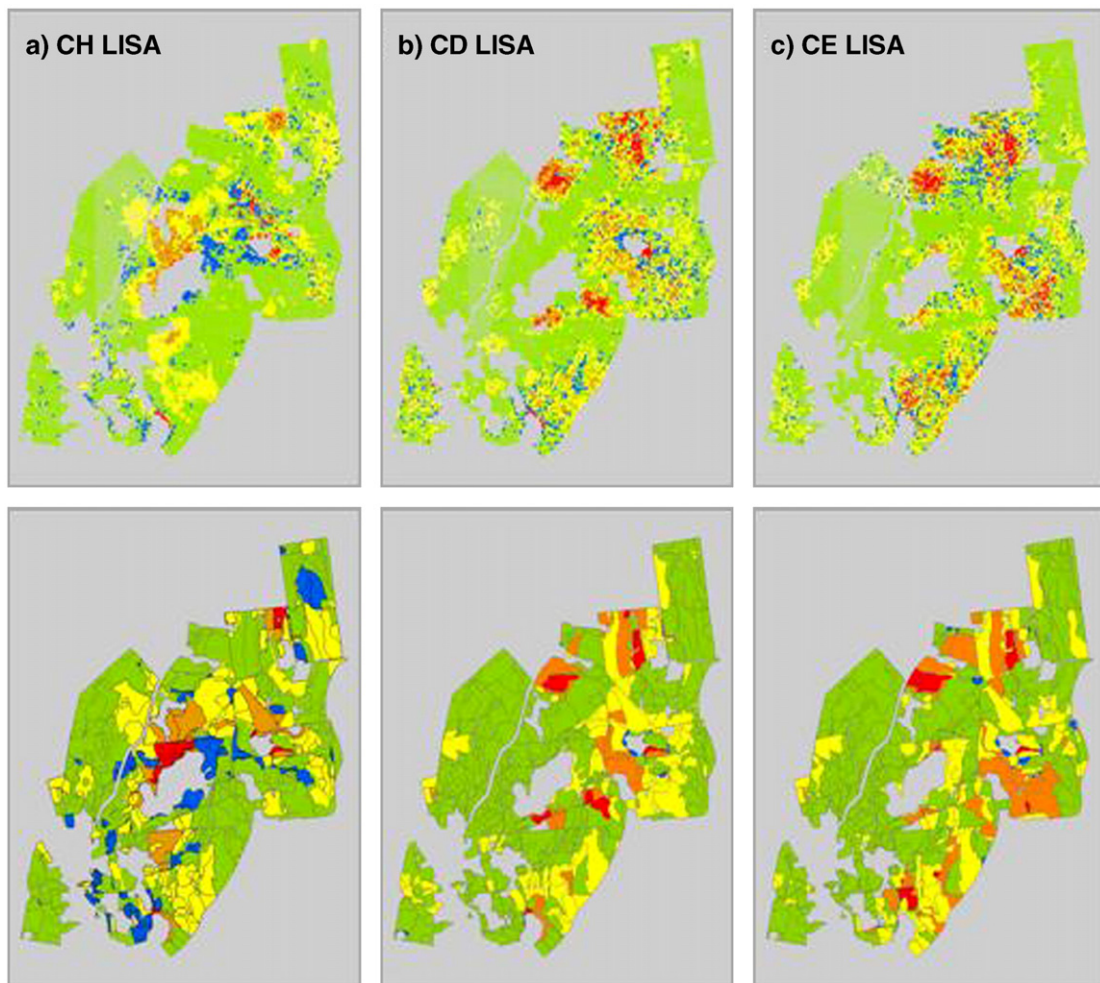

Fig. 8. Local autocorrelation measures for the different canopy properties for each footprint (above) and average LISA values for each damage class/predominant species polygon (below). Low values are blue; high values are red. Color classes follow Jenks natural breaks. (For interpretation of the references to color in this figure legend, the reader is referred to the web version of this article.)

or bin number bias from CD as the diversity index was significantly correlated to the number of occupied bins ($r^2 = 0.816$) and to a lesser extent height ($r^2 = 0.395$), CE remained significantly correlated with CH ($r^2 = 0.72$). Again when considered separately or together, the hurricane damage and predominant species classes contributed to significant ($P < 0.05$) differences in CD and CE measures derived by the LiDAR.

3.2. Patterns of global and local autocorrelation

All damage and species classes exhibited non-random patterns of canopy topography and internal canopy properties at lag distances below 100 m (Fig. 7). This scale of autocorrelation is on the order of those found in pixel to pixel variation of LAI classes at Harvard Forest by Tian et al. (2002). Though height differences were more apparent among the species classes than hurricane damage classes a visual inspection of the autocorrelation patterns shows the opposite. The correlogram for the most disturbed class had the highest autocorrelation values at smaller lag distances (i.e., < 150 m) whereas the least disturbed class had the lowest autocorrelation values after 40 m (Fig. 7a). The predominant species class correlograms were more convoluted than the hurricane damage class correlograms (Fig. 7b). The red pine dominated stands
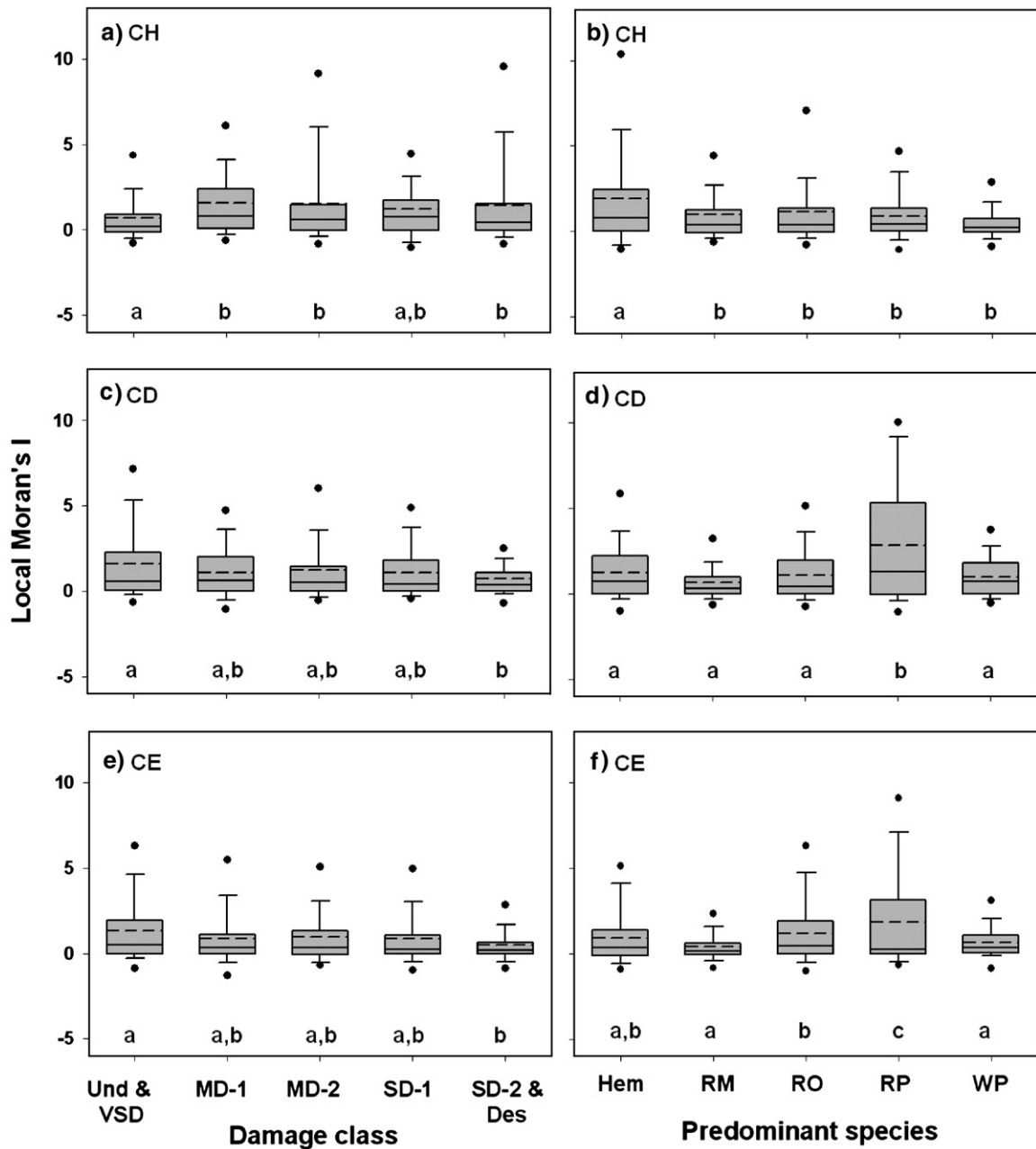

Fig. 9. Average LISA values for damage and predominant species classes by polygon. Dashed lines represent average values. Solid lines in boxes represent median values. Edges of boxes represent 25th and 75th percentiles. Whisker bars represent 10th and 90th percentiles. Circular markers represent 5th and 95th percentiles. For a given panel, different letters above a tic mark indicate statistically different values ($P < 0.05$ based on Duncan's post hoc test).

exhibited the highest autocorrelation values which may be explained by the regular spacing and fairly even aged properties of the plantation. Global autocorrelation levels were generally lower for CD and CE measures than CH measures. Patterns for the hurricane damage classes for CD and CE were somewhat reversed than found with CH; the least disturbed class had higher autocorrelation levels for CD and CE than the most disturbed class. The correlograms were the least smooth for the most disturbed class. Autocorrelation patterns for CD and CE were very similar among the dominant species classes.

With the aggregation of the footprint level LISA measures to the stand polygon level (Fig. 8), one can visualize the "hot spots" of local autocorrelation. From this, one can see that the spatial distribution of LISA values for CD and CE are generally similar, but differ for CH. The mean LISA values for the damage class polygons followed some of the behaviors exhibited among the correlograms (Fig. 9). For CH, the areas most damaged by the 1938 hurricane had higher average local autocorrelation values than the least damaged areas. This pattern was reversed for the CD and CE average LISA measures. The local auto-correlation measures did not seem to correspond to the global autocorrelation measures. Hemlock had higher local spatial autocorrelation levels with respect to CH than the other species indicating a consistent height for each hemlock dominated polygon. For CD and CE, red pine had the highest average LISA values. This again may relate to the even age properties and regular spacing of the red pine plantation.

4. Discussion

The subtle, yet significant differences in canopy heights and vertical profiles of the laser return among the damage classes suggest the forest canopy on the Prospect Hill tract had not completely recovered 65 years after the hurricane and the ensuing salvage operations. This is further evidenced by the differences in the global and local autocorrelation patterns among the canopy height measures. These all show the more severely disturbed stands to be shorter, with a less diverse vertical distribution of laser backscatter and higher levels of spatial autocorrelation for CH and lower levels of CD and evenness. Though not measured here, these changes in LVIS waveform properties resulting from the disturbance most likely correspond to different levels of biomass (Anderson et al., 2006) However, more conspicuous differences in canopy height and canopy height diversity are found when analyzing the predominant species classes across this patchy landscape. This is visually apparent by the diversity of canopy height profiles for the different predominant species classes.

The lower average canopy heights in the more heavily damaged stands may reflect the reduction in number or absence of taller trees or differential growth rates after the hurricane (Merrens & Peart, 1992). This may also relate to an earlier study (Motzkin et al., 1999) which found increases in basal area associated with lower levels of damage. The higher autocorre-lation patterns below 150 m and the lower CD metrics indicate that the canopy in the more damaged stands have not differ-entiated horizontally and vertically as those in the less damaged

stands. It is possible that the less damaged Harvard Forest canopies from the 1938 hurricane exhibited a more random spatial distribution of heights across scales <100 m, like the Duke Forest after the 1996 Hurricane Fran disturbance (Boutet & Weishampel, 2003), but have since recovered. Thus LiDAR, in a similar vein as optical and microwave sensors that are able to detect and age fire (Amiro & Chen, 2003; Bourgeau-Chavez et al., 2002) and microburst blowdowns (Nelson et al., 1994) scars was able to distinguish among hurricane damage classes. This synoptic approach may provide a different, more efficient approach than ground-based observations of canopy structure after a disturbance (e.g., Rhoads et al., 2004).

The fact that the canopy has not completely recovered after 65 years in this transition northern hardwood forest may not be unexpected as canopy structure in a tropical rainforest was found to recover more slowly than other ecosystem properties after a hurricane (Beard et al., 2005). The legacy of the hurricane as reflected by the canopy structure (i.e., CH and diversity) may have habitat ramifications for arboreal species notably birds (Hill et al., 2004; MacArthur & MacArthur, 1961) as it should relate to the foliage-height diversity index as found with eastern deciduous forests (Harding et al., 2001). As the canopy dictates other environmental conditions such as light penetration, differential understory environments should persist as a result of the hurricane. However, this is not reflected by the understory floral composition which had since recovered (Mabry & Korsgren, 1998) to its pre-hurricane state and was found not to be significantly influenced by the overstory (Motzkin et al., 1999). Most likely, the understory species composition is more of a function of microclimate effects that may be masked by the relatively coarse footprint of this LiDAR. As current understory composition on Prospect Hill reflects an array of historic land uses (Motzkin et al., 1999), these may also have contributed to existing canopy structural differences (Foster, 1992).

Over the last three centuries, the Prospect Hill tract has been exposed to repeated human- and natural-born disturbances. Though not examined here, historic agricultural uses have been shown to affect recovery after a hurricane in a tropical system (Uriarte et al., 2004). Given the subtle differences in canopy height, diversity, and evenness attributed to the 1938 hurricane, it seems unlikely that signs of earlier disturbances could be detected using this airborne LiDAR. However, the species that comprise the present Prospect Hill overstory are a function of 18th- and 19th-century land use patterns (see Motzkin et al., 2004). For example, hemlock dominated stands are found on sites that were not cleared at least since 1730; red maple stands are found on sites that were once woodlots and unimproved pastures; oak–maple associations are found primarily on sites that were once pastures and tilled fields; pine–oak associations are found on sites that were pastures and plowed fields. Thus, there should be indirect relationships among the LiDAR-derived canopy properties and historic land uses.

Acknowledgments

References

Aber, J. D. (1979). Foliage-height profiles and succession in northern hardwood forests. *Ecology*, *60*, 18−23.

Amiro, B. D., & Chen, J. M. (2003). Forest-fire-scar aging using SPOT-VEGETATION for Canadian ecoregions. *Canadian Journal of Forest Research*, *33*, 1116−1125.

Anderson, J., Martin, M. E., Smith, M. -L., Dubayah, R. O., Hofton, M. A., Hyde, P., et al. (2006). The use of waveform lidar to measure northern temperate mixed conifer and deciduous forest structure in New Hampshire. *Remote Sensing of Environment*, *105*, 248−261.

Anselin, L. (1995). Local indicators of spatial association — LISA. *Geographical Analysis*, *27*, 93−115.

Beard, K. H., Vogt, K. A., Vogt, D. J., Scatena, F. N., Covich, A. P., Sigurdardottir, R., et al. (2005). Structural and functional responses of a subtropical forest to 10 years of hurricanes and droughts. *Ecological Monographs*, *75*, 345−361.

Blair, J. B., Hofton, M. A., & Rabine, D. L. (2004). *Processing of NASA LVIS elevation and canopy (LGE, LCE and LGW) data products, version 1.0.* Available at: http://lvis.gsfc.nasa.gov

Blair, J. B., Rabine, D. L, & Hofton, M. A. (1999). The Laser Vegetation Imaging Sensor (LVIS): A medium-altitude, digitization-only, airborne laser altimeter for mapping vegetation and topography. *ISPRS Journal of Photogrammetry and Remote Sensing*, *54*, 115−122.

Birnbaum, P. (2001). Canopy surface topography in a French Guiana forest and the folded forest theory. *Plant Ecology*, *153*, 293−300.

Boose, E. R., Chamberlin, K. E., & Foster, D. R. (2001). Landscape and regional impacts of hurricanes in New England. *Ecological Monographs*, *71*, 27−48.

Boose, E. R., Foster, D. R., & Fluet, M. (1994). Hurricane impacts to tropical and temperate forest landscapes. *Ecological Monographs*, *64*, 369−400.

Boots, B. (2002). Local measures of spatial association. *Ecoscience*, *9*, 168−176.

Bourgeau-Chavez, L. L., Kasischke, E. S., Brunzell, S., Mudd, J. P., & Tukman, M. (2002). Mapping fire scars in global boreal forests using imaging radar data. *International Journal of Remote Sensing*, *23*, 4211−4234.

Boutet, J. C., & Weishampel, J. F. (2003). Spatial pattern analysis of pre- and post-hurricane forest canopy structure. *Landscape Ecology*, *18*, 553−559.

Bowers, W. W., Franklin, S. E., Hudak, J., & McDermid, G. J. (1994). Forest structural damage analysis using semivariance. *Canadian Journal of Remote Sensing*, *20*, 28−36.

Cohen, W. B., Spies, T. A, & Bradshaw, G. A. (1990). Semivariograms of digital imagery for analysis of conifer canopy structure. *Remote Sensing of Environment*, *34*, 167−178.

Dale, M. R. T., Dixon, P., Fortin, M. J., Legendre, P., Myers, D. E., & Rosenberg, M. S. (2002). Conceptual and mathematical relationships among methods for spatial analysis. *Ecography*, *25*, 558−577.

Drake, J. B., & Weishampel, J. F. (2000). Multifractal analysis of canopy height measures in a longleaf pine savanna. *Forest Ecology and Management*, *128*, 121−127.

Foster, D. R. (1988). Species and stand response to catastrophic wind in central New England, USA. *Journal of Ecology*, *76*, 135−151.

Foster, D. R. (1992). Land-use history (1730–1990) and vegetation dynamics in central New England, USA. *Journal of Ecology*, *80*, 753−772.

Foster, D. R., & Boose, E. R. (1992). Patterns of forest damage resulting from catastrophic wind in central New England, USA. *Journal of Ecology*, *80*, 79−98.

Foster, D. R., Aber, J. D., Melillo, J. M., Bowden, R. D., & Bazzaz, F. A. (1997). Forest response to disturbance and anthropogenic stress. *Bioscience*, *47*, 437−445.

Foster, D., Cooper-Ellis, S., Barker Plotkin, A., Carlton, G., Bowden, R., MaGill, A., et al. (2004). Simulating a catastrophic hurricane. In D. Foster & J. Aber (Eds.), *Forests in time* (pp. 235−258). New Haven, Connecticut: Yale University Press.

Foster, D. R., Knight, D. H., & Franklin, J. F. (1998). Landscape patterns and legacies resulting from large, infrequent forest disturbances. *Ecosystems*, *1*, 497−510.

Franklin, J. F., Spies, T. A., Van Pelt, R., Carey, A. B., Thornburgh, D. A., Rae Berg, D., et al. (2002). Disturbances and structural development of natural forest ecosystems with silvicultural implications, using Douglas-fir forests as an example. *Forest Ecology and Management*, *155*, 399−423.

Frazer, G. W., Wulder, M. A., & Niemann, K. O. (2005). Simulation and quantification of the fine-scale spatial pattern and heterogeneity of forest canopy structure: a lacunarity-based method designed for analysis of continuous canopy heights. *Forest Ecology and Management*, *214*, 65−90.

Gamma Design. (2005). *GS+ Version 7. Geostatistics for the environmental sciences.* MI: Plainwell (160 pp).

Getis, A., & Ord, J. K. (1996). Local spatial statistics: An overview. In P. Longley & M. Batty (Eds.), *Spatial analysis: modelling in a GIS environment* (pp. 261−277). Cambridge: GeoInformation International.

Hallé, F., Oldeman, R. A. A., & Tomlinson, P. B. (1978). *Tropical trees and forests: An architectural analysis.* New York: Springer-Verlag.

Harding, D. J., Lefsky, M. A., Parker, G. G., & Blair, J. B. (2001). Laser altimeter canopy height profiles: Methods and validation for closed-canopy, broadleaf forests. *Remote Sensing of Environment*, *76*, 283−297.

Harvard Forest LTER. (2005). *Harvard Forest long term ecological research site.* Available at: http://harvardforest.fas.harvard.edu/

Hashimoto, H., Imanishi, J., Hagiwara, A., Morimoto, Y., & Kitada, K. (2004). Estimating forest structure indices for evaluation of forest bird habitats by an airborne laser-scanner. In M. Thies, B. Kohn, H. Spiecker, & H. Weinacker (Eds.), *Proceedings of the ISPRS working group VIII/2 laser-scanners for forest and landscape assessment* (pp. 254−257). Germany: Freiburg.

Hill, R. A., Hinsley, S. A., Gaveau, D. L. A., & Bellamy, P. E. (2004). Predicting habitat quality for Great Tits (*Parus major*) with airborne laser scanning data. *International Journal of Remote Sensing*, *25*, 4851−4855.

Hofton, M. A., Rocchio, L. E., Blair, J. B., & Dubayah, R. (2002). Validation of Vegetation Canopy Lidar sub-canopy topography measurements for a dense tropical forest. *Journal of Geodynamics*, *34*, 491−502.

Hyde, P., Dubayah, R., Peterson, B., Blair, J. B., Hofton, M., Hunsaker, C., et al. (2005). Mapping forest structure for wildlife habitat analysis using waveform lidar: Validation of montane ecosystems. *Remote Sensing of Environment*, *96*, 427−437.

Keeton, W. S., & Franklin, J. F. (2005). Do remnant old-growth trees accelerate rates of succession mature Douglas-fir forests? *Ecological Monographs*, *75*, 103−118.

King, D. J., Olthof, I., Pellikka, P. K. E., Seed, E. D., & Buston, C. (2005). Modelling and mapping damage to forests from an ice storm using remote sensing and environmental data. *Natural Hazards*, *35*, 321−342.

Leak, W. B. (1983). *Stocking, growth, and habitat relations in New Hampshire hardwoods*. Forest Service—U.S. Department of Agriculture. Northeastern Forest Experiment Station. NE-523.

Lefsky, M. A., Harding, D., Cohen, W. B., Parker, G., & Shugart, H. H. (1999). Surface lidar remote sensing of basal area and biomass in deciduous forests of eastern Maryland, USA. *Remote Sensing of Environment*, *67*, 83−98.

Lefsky, M. A., Harding, D. J., Keller, M., Cohen, W. B., Carabajal, C. C., Espirito-Santo, F. D., et al. (2005). Estimates of forest canopy height and aboveground biomass using ICESat. *Geophysical Research Letters*, *32* Art. No. L22S02.

Legendre, P. (1993). Spatial autocorrelation: trouble or new paradigm? *Ecology*, *74*, 1659−1673.

Lévesque, J., & King, D. J. (1999). Airborne digital camera image semivariance for evaluation of forest structural damage at an acid mine site. *Remote Sensing of Environment*, *68*, 112−124.

Levine, N. (2004). *CrimeStat III: A spatial statistics program for the analysis of crime incident locations.* Washington, DC: The National Institute of Justice.

Lindenmayer, D. B., Foster, D. R., Franklin, J. F., Hunter, M. L, Noss, R. F., Schmiedelow, F. A., et al. (2004). Salvage harvesting policies after natural disturbance. *Science*, *303*, 1303.

Mabry, C., & Korsgren, T. (1998). A permanent plot study of vegetation and vegetation-site factors fifty-three years following disturbance in central New England, USA. *Ecoscience*, *5*, 232−240.

MacArthur, R. H., & MacArthur, J. W. (1961). On bird species diversity. *Ecology*, *42*, 594−598.

McElhinny, C., Gibbons, P., Brack, C., & Bauhus, J. (2005). Forest and woodland stand structural complexity: Its definition and measurement. *Forest Ecology and Management*, *218*, 1−24.

McMaster, K. J. (2005). Forest blowdown prediction: A correlation of remote sensed contributing factors. *Northern Journal of Applied Forestry*, *22*, 48−53.

Merrens, E. J., & Peart, D. R. (1992). Effects of hurricane damage on individual growth and stand structure in a hardwood forest in New Hampshire, USA. *Journal of Ecology*, *80*, 787−795.

Motzkin, G., Foster, D., Allen, A., Donohue, K., & Wilson, P. (2004). Forest landscape patterns, structure, and composition. In D. Foster & J. Aber (Eds.), *Forests in time* (pp. 171−188). New Haven, Connecticut: Yale University Press.

Motzkin, G., Wilson, P., Foster, D. R., & Allen, A. (1999). Vegetation patterns in heterogeneous landscapes: The importance of history and environment. *Journal of Vegetation Science*, *10*, 903−920.

Nadkarni, N. M., Parker, G. G., Ford, E. D., Cushing, J. B., & Stallman, C. (1996). The international canopy network: A pathway for interdisciplinary exchange of scientific information on forest canopies. *Northwest Science*, *7*, 104−108.

Nelson, B. W., Kapos, V., Adams, J. B., Oliveira, W. J., Braun, O. P. G., & do Amaral, I. L. (1994). Forest disturbance by large blowdowns in the Brazilian Amazon. *Ecology*, *75*, 853−858.

Palik, B., & Robl, J. (1999). *Structural legacies of catastrophic windstorm in a mature great lakes aspen forest*. Forest Service − U.S. Department of Agriculture. North Central Research Station. NC-337.

Parker, G. G., & Brown, M. J. (2000). Forest canopy stratification—Is it useful? *The American Naturalist*, *155*, 473−484.

Parker, G. G., Harmon, M. E., Lefsky, M. A., Chen, J., Van Pelt, R., Weiss, S. B., et al. (2004). Three-dimensional structure of an old-growth Pseudotsuga-tsuga canopy and its implications for radiation balance, microclimate, and gas exchange. *Ecosystems*, *7*, 440−453.

Popescu, S. C., Wynne, R. H., & Scrivani, J. A. (2004). Fusion of small-footprint lidar and multispectral data to estimate plot-level volume and biomass in deciduous and pine forests in Virginia, USA. *Forest Science*, *50*, 551−565.

Rhoads, A. G., Hamburg, S. P., Fahey, T. J., Siccama, T. G., & Kobe, R. (2004). Comparing direct and indirect methods of assessing canopy structure in a northern hardwood forest. *Canadian Journal of Forest Research*, *34*, 584−591.

Rowlands, W. (1941). Damage to even-aged stands in Petersham, Massachusetts, by the 1938 hurricane as influenced by stand condition. Thesis paper for Master of Forestry degree, Harvard University, Cambridge Massachusetts.

Smith, B., & Wilson, J. B. (1996). A consumer's guide to evenness indices. *Oikos*, *76*, 70−82.

Spies, T., & Cohen, W. B. (1992). An index of canopy height diversity. *Coastal Oregon Productivity Enhancement Program (COPE) Report*, *Vol. 5* (pp. 5−7).

Spurr, S. H. (1956a). Forest associations in the Harvard Forest. *Ecological Monographs*, *26*, 245−262.

Spurr, S. H. (1956b). Natural restocking of forests following the 1938 hurricane in central New England. *Ecology*, *37*, 443−451.

Tian, Y., Woodcock, C. E., Wang, Y., Privette, J. L., Shabanov, N. V., Zhou, L., et al. (2002). Multiscale analysis and validation of the MODIS LAI product II. Sampling strategy. *Remote Sensing of Environment*, *83*, 431−441.

Tunick, A. (2003). Calculating the micrometeorological influences on the speed of sound through the atmosphere in forests. *Journal of the Acoustical Society of America*, *114*, 1796−1806.

Turner, M. G., & Dale, V. H. (1998). Comparing large, infrequent disturbances: What have we learned. *Ecosystems*, *1*, 493−496.

Turner, M. G., Baker, W. L., Peterson, C. J., & Peet, R. K. (1998). Factors influencing succession: Lessons from large, infrequent natural disturbances. *Ecosystems*, *1*, 511−523.

Unruh, J. D. (1991). Canopy structure in natural and agro-forest successions in Amazonia. *Tropical Ecology*, *32*, 168−181.

Uriarte, M., Rivera, L. W., Zimmerman, J. K., Aide, T. M., Power, A. G., & Flecker, A. S. (2004). Effects of land use history on hurricane damage and recovery in a neotropical forest. *Plant Ecology*, *174*, 49−58.

Weishampel, J. F., Blair, J. B., Dubayah, R., Clark, D. B., & Knox, R. G. (2000). Canopy topography of an old-growth tropical rain forest landscape. *Selbyana*, *21*, 79−87.

Weishampel, J. F., Urban, D. L., Shugart, H. H., & Smith Jr., J. B. (1992). Semivariograms from a forest transect gap model compared with remotely sensed data. *Journal of Vegetation Science*, *3*, 521−526.

Westveld, M., Ashman, R. I., Baldwin, H. I., Holdsworth, R. P., Johnson, R. S., Lambert, J. H., et al. (1956). Natural forest vegetation zones of New England. *Journal of Forestry*, *54*, 332−338.

Wulder, M., & Boots, B. (2001). Local spatial autocorrelation characteristics of Landsat TM imagery of a managed forest area. *Canadian Journal of Remote Sensing*, *27*, 67−75.